Synthesis of Maleic Acid from Biomass-Derived Furfural in the Presence of KBr/Graphitic Carbon Nitride (g-C_3N_4) Catalyst and Hydrogen Peroxide

Tao Yang,[a] Wenzhi Li,[a,b,*] Qingchuan Liu,[c] Mingxue Su,[a] Tingwei Zhang,[a] and Jianru Ma [a]

A one-step, liquid-phase hydrogen peroxide reaction system, which was heterogeneously catalyzed by KBr-doped graphitic carbon nitride (KBr/g-C_3N_4), was developed for the conversion of furfural to maleic acid (MA). At first, a 68.0% MA yield was achieved in a homogeneous reaction system catalyzed by KBr-KOH. Next, a series of K-doped g-C_3N_4 catalysts with various potassium salts (KBr, KCl, KNO_3, and KOH) was synthesized and tested for the conversion of furfural to MA, 2-buten-1,4-olide (FRO), and succinic acid (SA). When comparing the various K-doped g-C_3N_4 catalysts, KBr/g-C_3N_4 enhanced MA selectivity, which resulted in complete furfural conversion and a 70.4% MA yield (at 100 °C for 180 min). Furthermore, a synergistic interaction was observed between KBr and the g-C_3N_4 support, which could explain why KBr/g-C_3N_4 had the highest MA selectivity.

Keywords: Furfural oxidation; KBr/graphic carbon nitride (g-C_3N_4); Maleic acid; Synergistic effect

Contact information: a: Laboratory of Basic Research in Biomass Conversion and Utilization, Department of Thermal Science and Energy Engineering, University of Science and Technology of China, Hefei 230026, P. R. China; b: National Synchrotron Radiation Laboratory, University of Science and Technology of China, Hefei 230026, P. R. China.; c: Hefei University of Technology, School of Biological and Medical Engineering, No. 193 Tunxi Road, Baohe District, Hefei, Anhui 230009, PR China;
** Corresponding author: liwenzhi@ustc.edu.cn*

INTRODUCTION

Maleic acid (MA), as an important chemical intermediate; it is widely used by chemical manufactures to produce resins, lubricant additives, surface coatings, vinyl co-polymers, and agricultural chemicals (Roa Engel *et al.* 2008). It has an industrial demand of up to 1,800,000 tons per year (Wojcieszak *et al.* 2015). Maleic acid is industrially produced from the aerobic oxidation of butane, benzene, and butadiene, which are derived from petroleum oil, which has environmental issues (Guo and Yin 2011; Araji *et al.* 2017). In this regard, an alternative method was developed to achieve a simple and efficient reaction route for MA production. Furfural is an organic intermediate that is derived from biomass sources, such as corncob, corn stover, wheat bran, oat, straw, and sawdust (Xu *et al.* 2018; Zhang *et al.* 2016). The wide and renewable availability of furfural makes it a great resource for selectively producing MA (Du *et al.* 2011; Li *et al.* 2016).

Currently, the production of MA from furfural has been reported using various gas-phase and liquid-phase catalytic oxidation systems. In the field of catalytic aerobic oxidation of furfural, Guo and Yin (2011) reported that phosphomolybdic acid catalyst had 50.4% furfural conversion and 34.5% MA yield when used at optimum reaction conditions; the authors used an aqueous/organic bi-phasic medium, where the oxidation occurred in

the aqueous phase, whereas the organic phase contained the furfural and gradually released it to the aqueous phase as it was consumed. Li *et al.* (2016a) developed a heterogeneous catalytic system that used Mo-V metal oxides as a catalyst to achieve a 65% MA yield when using an acetic acid medium and an oxygen atmosphere at 120 °C for 12 h. These investigators demonstrated that the reaction medium played a crucial role with respect to the performance of the catalyst. Alonso-Fagundez *et al.* (2012) observed a maximum 70% maleic anhydride yield from furfural using selective gas-phase oxidation at 320 °C with a VOx/Al_2O_3 catalyst. Other researchers have investigated the production of MA from furfural using hydrogen peroxide in a liquid-phase medium. However, it is a very complicated to produce MA from furfural with H_2O_2 as an oxidant because of the presence of two oxidizable functional groups of furfural (C=C and C=O groups) (Kul'nevich and Badovskaya 1975). Choudhary *et al.* (2013) studied the catalytic aerobic oxidation of furfural to succinic acid (SA) and MA using Amberlyst-15 resin as a catalyst, which demonstrated that sulfonic acid groups, as well as sulfonyl groups, in the resin can affect the catalytic activity. Li *et al.* (2016b) established a simplified reaction network to analyze the solvent effect; furthermore, they optimized the product yield by changing the catalyst/furfural molar ratio, furfural concentration, and reaction temperature. The authors proposed a possible reaction pathway whereby the formic acid reacted with hydrogen peroxide to produce performic acid, which acted as the oxidant in the bi-phasic reaction medium. Based on the result of Li *et al.* (2016b), an enhanced reaction system was proposed by Li *et al.* (2017), who observed 95% MA yield when using formic acid as the catalyst, H_2O_2 as the oxidant, and furfural as the substrate (Li *et al.* 2017). However, the extra water added into the above system reduced the MA yield considerably. For example, when a 1:3 formic acid-to-water ratio was used, the MA yield was only 13%. Araji *et al.* (2017) reported the successful furfural conversion to maleic and fumaric acid (> 90% yield) when using betaine hydrochloride as the catalyst. In addition to furfural as the substrate for MA and maleic anhydride production, some investigators have examined glucose as a substrate for succinic acid production (Podolean *et al.* 2016; Rizescu *et al.* 2017).

In addition, there has been some discussion about the possible mechanism of furfural oxidation to MA. Some studies have demonstrated that furoic acid (FA) is an important intermediate in the furfural oxidation reaction; furoic acid can undergo a decarboxlation reaction to form furan, which can then be oxidized by H_2O_2 to generate C4 products (Badovskaya *et al.* 2014). However, Danon *et al.* (2013) proposed that 2-formyloxyfuran is the crucial intermediate. Xiang *et al.* (2016) investigated the oxidation of furfural with H_2O_2 and H_2O_2-$Mg(OH)_2$ systems; the authors proposed that the addition of $Mg(OH)_2$ improves the selectivity of 2-buten-1,4-olide (44.8%) and succinic acid (38.0%) yields with the complete conversion of the furfural substrate. Furthermore, the oxidation of the ring of furfural is suppressed by synergistic interactions between Mg^{2+} and HO^- ions, where HO^- helps to ionize H_2O_2 to form HOO^-; the generated HOO^- attacks the carbonyl group of the furan ring instead of the carbon-carbon double bond. Alonso-Fagundez *et al.* (2014) used titanium silicalite (TS-1) as a catalyst and H_2O_2 as an oxidant to achieve 80% MA yield. These authors proposed an epoxidation mechanism for the furan ring with the subsequent release of formic acid. In fact, a detailed reaction mechanism requires further efforts, which will be a direction for future studies.

Based on a large number of related reports on the synthesis of MA, the major drawbacks of homogeneous system are the required product-catalyst separation, low MA

selectivity, and difficulty in recycling. And inspired by the function of HO^- postulated in the report of Xiang *et al.* (2016), a new catalytic reaction system using KBr and HO^- as a combined catalyst system was explored for the oxidation of furfural to MA. Furthermore, it is known that homogeneous catalysts are difficult to recover. Thus, a novel heterogeneous catalyst composed of the Brønsted base graphitic carbon nitride (g-C_3N_4) (Lin *et al.* 2016) with KBr was designed and subsequently used to convert furfural into MA. A comprehensive study was carried out to explain the remarkable catalytic activity for MA production of the KBr/ g-C_3N_4 catalyst.

In this study, to intensify the production of MA, a novel KBr/g-C_3N_4 catalyst was employed, and the results indicated that the presence of KBr and the support of g-C_3N_4 are beneficial for selective synthesis of MA. A catalytic system (water and H_2O_2) was applied as solvent that embodied the characteristic of green chemistry. Furthermore, the effects of reaction conditions including reaction temperature, water contents, retention time, catalyst species, and structure of substrate were investigated.

EXPERIMENTAL

Materials

KBr, KNO_3, KCl, KOH, NaOH, NaBr, H_2O_2, and urea were purchased from Sinopharm Chemical Reagent Co., Ltd. (Shanghai, China). Maleic acid, 2-buten-1,4-olide (2(5H)-Furanone, FRO), succinic acid, furfural, 5-hydroxymethyl furfural, and 2-furoic acid were obtained from Aladdin (Shanghai, China). All chemicals were used as received without further purification.

Catalyst Preparation

Graphitic carbon nitride (g-C_3N_4) was prepared by the method of Zhang *et al.* (2012) with slight modifications. Urea powder (10 g) was added to a crucible. Next, the crucible was covered and placed in a muffle furnace. The furnace was heated to 550 °C from room temperature at a speed of 5 °C /min. The furnace temperature was kept at 550 °C for 4 h. Afterwards, the covered crucible was removed from the furnace and cooled to room temperature.

The KBr/g-C_3N_4 was prepared in a similar manner as the above g-C_3N_4. KBr (0.5 g), urea (10 g), and distilled water (30 mL) were mixed at room temperature; the solution was dried in an oven at 80 °C overnight. Afterwards, the dried mixture was calcined in a covered crucible in a muffle furnace at 550 °C for 4 h, which was heated from room temperature at a rate of 5 °C /min. Afterwards, the crucible was removed from the furnace and cooled to room temperature

The regeneration of the spent KBr/g-C_3N_4 catalyst was accomplished by mixing the recovered KBr/g-C_3N_4 (1 g) with KBr (50 mg) and deionized water (30 mL) at room temperature. This mixture was dried and calcined using the same method as described for the original KBr/g-C_3N_4 catalyst.

TiO_2 and CeO_2 were doped with K in accordance with the method of Wang *et al.* (2017) and Takase *et al.* (2014) with some modifications. A solution was made by mixing KBr (0.1 g), TiO_2 (2 g), and deionized water (30 mL) at 600 rpm for 24 h; the resulting solution was dried in an oven at 80 °C. Afterwards, the dried solid was calcined at 550 °C

using the same method described for the KBr/g-C_3N_4 catalyst. The calcined catalyst was ground and stored in a drying vessel until needed. The K-doped CeO_2 catalyst was made using the same procedure as that for the K-doped TiO_2 catalyst.

Experimental Method

The catalytic reaction of furfural was used to test the catalytic ability of laboratory-made catalysts. Typically, the experiments were performed in a sealed thick-walled glass tube (15 mL). To this tube was added furfural (96 mg), catalyst (50 mg), H_2O_2 (1 mL), and distilled water (2 mL). Then, the tube was heated to a given reaction temperature and maintained at that temperature for a specified time in a preheated oil bath. The glass tube was then cooled to room temperature when the reaction was complete. Finally, the resulting products were separated from the solid catalyst by filtration and stored at 4 °C prior to analysis.

To evaluate the catalytic activity of potassium cations, the hot-filtration experiment was carried out and as follows: 100 mg KBr/g-C_3N_4 and 4 mL distilled water were heated at 100 ℃ for 3 h. The catalyst and filtrates are separated by filtration. Then 2 mL filtrate, 1 mmol furfural and 1 mL H_2O_2were added into thick-walled glass tube and reacted at 100 ℃ for 3 h. Furthermore, the above catalyst was dried at oven and also used to analyze the catalytic activity: 50 mg catalyst, 2 mL distilled water, 1 mmol furfural and 1 mL H_2O_2 were heated at 100 ℃ for 3 h.

Characterization of Catalyst

The morphologies and structural features of the catalysts were characterized by transmission electron microscopy (TEM) (JEM-2010Plus TEM, JEOL USA; Peabody, MA, USA) and by TEM-energy dispersive X-ray spectroscopy (TEM-EDS). X-ray diffraction (XRD) was used to determine the crystallinity of the samples with Cu Kα radiation. The alkali measurement of K-doped g-C_3N_4 was performed using CO_2-temperature programmed desorption (CO_2-TPD) (Quantachrome Instruments; Boynton Beach, FL, USA). Fourier-transform infrared (FTIR) spectra were recorded on a Nicolet 8700 instrument (Thermo Fisher Scientific; Waltham, MA, USA); samples were pressed with KBr into disks, which were then scanned. BET surface areas of samples were measured by N_2 adsorption-desorption isothermal (-196 ℃) on Tristar II 3020M (Micromeritics Instruments, American).

Analysis of Products

The high-performance liquid chromatography (HPLC) analysis of the reaction products was performed with a Waters HPLC 515 pump (Waters; Milford, MA, USA) equipped with a Waters 2414 refractive index detector and Bio-Rad Aminex HPX-87H column. The analysis methods are used according to the work of Choudhary et al. (2013) with some modifications. The mobile phase was an aqueous 5 mM H_2SO_4 solution; an elution rate of 0.6 mL min^{-1} (60 ℃) was used. The conversion and yield were calculated using a calibration curve. An HPLC retention time (Fig. S1, Supplementary Information (SI), see Appendix) of 8.053 min was observed for maleic acid (MA), 11.139 min was observed for succinic acid (SA), 12.192 min was observed for furfural, and 26.467 min was observed for 2-buten-1,4-olide (FRO). The yields of MA, FRO and furfural were calculated according to Fig. S2 (SI) and the following equations:

$$furfural\ convversion = \left(1 - \frac{moles\ of\ furfural\ in\ products}{moles\ of\ starting\ furfural}\right) \times 100\% \quad (1)$$

$$product\ yield = \frac{moles\ of\ product\ produced}{moles\ of\ starting\ furfural} \times 100\% \quad (2)$$

where the "product" is either MA, SA or FRO.

RESULTS AND DISCUSSION

Catalyst Characterization

A series of K-doped g-C_3N_4 specimens was prepared with various potassium salts and urea. The FTIR spectra (Fig. 1) of the g-C_3N_4 and K-doped g-C_3N_4 exhibited the same peak at 2177 cm^{-1}, which is attributed to the cyano (-C≡N) group, which arose from the incomplete conversion of urea to g-C_3N_4 during calcination (Gao *et al.* 2013). Furthermore, the peak at 810 cm^{-1} is assigned to the bending vibration of s-triazine rings. The broad absorption band around 3000 to 3300 cm^{-1} originated from stretching vibrations of N-H and O-H bonds (Yang *et al*. 2017).

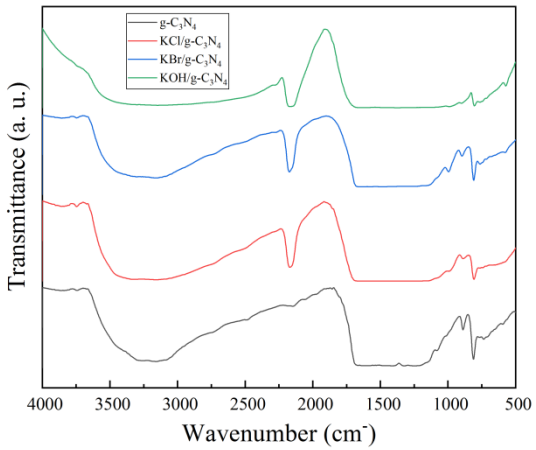

Fig. 1. FTIR spectra of pure g-C_3N_4 and K-doped g-C_3N_4 with various potassium salts

The XRD pattern (Fig. 2) was used to characterize the solid phase structure of pure g-C_3N_4, KOH/g-C_3N_4, KCl/g-C_3N_4, and KBr/g-C_3N_4. The peak at 27.4° in the diffraction patterns can be attributed to the (002) crystalline plane. This peak originates from the periodic interlayer stacking of conjugated aromatic structures along the c-axis, which is typical for graphitic layered structures. The intensity of the (002) peaks for the K-doped samples was less pronounced than it was for the pure g-C_3N_4. Furthermore, the (002) peak of K-doped g-C_3N_4 displayed a small 2θ shift. Pure KBr exhibits several well-defined peaks at 23°, 27°, 39°, 46° and 58°, which indicate the crystalline nature of KBr. For KBr/g-C_3N_4, the XRD patterns display a combination of the two sets of diffraction data for both g-C_3N_4 and KBr. The new peak in the XRD results of KBr/g-C_3N_4 are mainly caused by KBr. When KBr was doped with g-C_3N_4, the peaks of KBr appeared and the (002) peak of g-C_3N_4 became sharp. The KCl/g-C_3N_4 and KBr/g-C_3N_4 followed similar trends: with the addition of KBr and KCl, the characteristic peaks of g-C_3N_4 became weaker, and the

intensities of KX (X=Br, Cl) peaks became more prominent. The diffraction peaks at various 2θ values for the K-doped samples were indexed to the crystalline planes of the corresponding pure potassium salt (Zhang *et al.* 2015).

Figure 3 shows the TEM images of samples, which reveal the typical wrinkle structure for g-C_3N_4 and KBr/g-C_3N_4. Furthermore, as shown in Fig. S3 (SI), C and N elements can be observed in the g-C_3N_4, while KBr/g-C_3N_4 presented C, N, K, Br, and O elements. The presence of O indicates the incomplete conversion of urea to g-C_3N_4 during calcination. These observations correspond to the findings from XRD characterization. Meanwhile, the EDS mapping analysis of KBr/g-C_3N_4 indicates that K and Br element are uniformly distributed within the g-C_3N_4 support. Moreover, the alkalinity of the KBr/g-C_3N_4 catalyst (1.61 mmol/g) was almost the same as that of the original g-C_3N_4 (1.67 mmol/g) (Table S1, SI).

Furthermore, the specific surface areas of pure g-C_3N_4 and KBr doped g-C_3N_4 were also investigated. As shown in Table S1, the specific surface area of pure g-C_3N_4 was determined to be 220.1 ㎡/g, which is much higher than that KBr doped g-C_3N_4 (13.2 ㎡/g). The pure urea precursor can generate gas easy during heating treatment which can result in large specific areas (Cui *et al*. 2017). With the adding of KBr, the lower surface areas may imply that the KBr has been loaded into the support of g-C_3N_4.

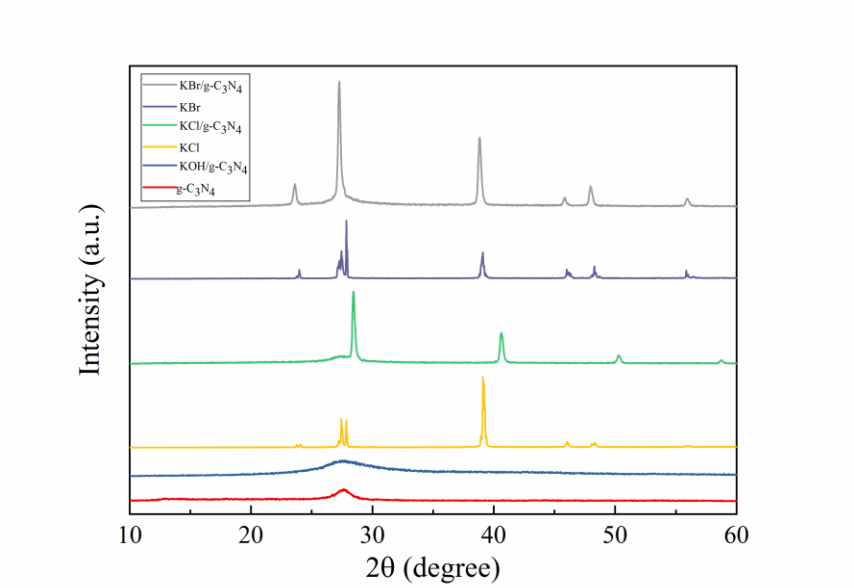

Fig. 2. XRD of pure g-C_3N_4, KOH/g-C_3N_4, KCl, KCl/g-C_3N_4, KBr, and KBr/g-C_3N_4

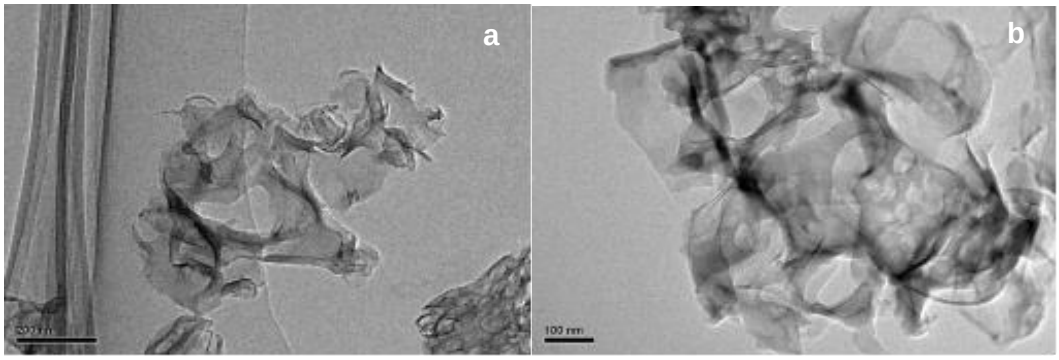

Fig. 3. Representative TEM images of: a) g-C_3N_4, and b) KBr/g-C_3N_4

Production of MA, FRO, and SA from Furfural Catalyzed by Various Catalysts

The effects of different catalysts for the conversion of furfural to MA, FRO, and SA are listed in Table 1. It is known that furfural oxidation by H_2O_2 to MA is very complicated and generates other side products, such as FRO, 2-furoic acid (FA), SA, and formic acid (Danon *et al.* 2013). When KBr was used as catalyst, complete furfural conversion and 31.0% MA yield could be detected. Moreover, there was no FRO or SA produced. In comparison with the KBr, a 37.1% MA yield, 23.3% FRO yield, and a 20.6% SA were observed with KOH (Table 1, entry 2) as the catalyst; whereas the yields of MA, FRO and SA were 12.2%, 25.2%, and 27.7% respectively by using KNO_3 (Table 1, entry 3) as the catalyst; and 23.0% MA yield, 3.6% FRO yield, and 8.4% SA were observed when using KCl (Table 1, entry 4) as the catalyst. The above results indicated that the presence of KBr may inhibit the reaction to FRO and SA.

Furthermore, when some KOH was added to the KBr catalytic system, the MA yield increased from 31.0% to 68.0% without any SA and FRO being produced (Entry 5 in Table 1). Possibly, this may be ascribed to the synergistic interaction between KBr and KOH. KOH can ionize H_2O_2 to form HOO^-. Then, HOO^- can react with the carbonyl group of furfural through the nucleophilic addition reaction to yield 2-perfuroic acid. Conversely, SA and FRO were not observed in the reaction products when KBr was used; hence, KBr may suppresses the SA/FRO side reactions.

To investigate what ion has an effect on the oxidation of furfural to MA, various inorganic salts were also investigated. The results are shown and compared in Table 1 (Entries 6 to 8). 36.1% MA, 21.5% FRO, and 3.3% SA yield were achieved with NaOH as catalyst (entry 6). The MA yield was 32.3% when NaBr (50 mg) and NaOH (50 mg) were used as the catalyst, whereas 61.9% MA yields were observed with KBr (25 mg) and NaOH (25 mg) (Table1, entry 7) as catalysts. Moreover, the ratios of KBr and NaOH were considered in Fig. S7 and KBr-NaOH (75 mg-25 mg) showed the best MA yield (66.2%), which indicated that the catalyst contents played a vital role in furfural oxidation and MA yield. Hence, the presence of KBr and OH^- were necessary to increase MA selectivity. Therefore, there is a synergism between KBr and HO^- that promotes MA formation. Based on these observations, the combination of KBr with g-C_3N_4 was designed, where the N atoms act as a Brønsted base (which was confirmed by TPD-CO_2 analysis; Table S1, SI). In previous reports, g-C_3N_4 was used in some alkali-catalyzed reactions where amino groups (including -NH_2 and -NH- groups) occurred at the edges of g-C_3N_4 (Su *et al.* 2010; Samanta and Srivastava 2017). The solid catalyst KBr/g-C_3N_4 was tested, and it resulted in

a 70.4% MA yield (Entry 9 in Table 1). At the same time, a series of K-doped g-C_3N_4 catalysts (made with KNO_3, KOH, and KCl) was prepared and used for the oxidation of furfural. The results (Entries 10 to 14 in Table 1) illustrate that the MA selectivities were lower, as MA, FRO, and SA are generated simultaneously. Specifically, A 16.2% MA yield, 30.6% FRO, and 44.1% SA were observed when using KOH/g-C_3N_4 (Table 1 entry 12) as the catalyst; whereas the yields were 21.1% MA, 26.2% FRO, and 22.4% SA by using KCl/g-C_3N_4 (Table 1 entry 13) as the catalyst; and the yields were 13.3% MA, 27.5% FRO, and 32.6% SA with KNO_3/g-C_3N_4 (Table 1 entry 14) as catalyst.

Based on the above results, a synergism between KBr and g-C_3N_4 support was observed, whereas other potassium salts, such as KCl, KOH, and KNO_3, did not enhance MA selectivity. Thus, a possible role of KBr/g-C_3N_4 is proposed for the conversion of furfural to MA (Fig. S6, SI). The g-C_3N_4 support can be used as a Brønsted base to ionize H_2O_2 to produce HOO^- in solution. Meanwhile, the K^+ of KBr/g-C_3N_4 may interact with the O atom of the furfural carbonyl group to enhance the electropositivity of carbonyl carbon and the Br^- may damage the conjugation of the furan ring and carbonyl carbon group. This makes the carbonyl more susceptible to HOO^- attack to form 2-perfuroic acid (Zhang *et al*. 2011). 2-Perfuroic is unstable and can be converted to 2-formyloxyfuran and hydroxyfuran. The hydroxyfuran may underwent rearrangement to intermediate A with the presence of bromide anion and furan ring opening would be happened. Then intermediate A can be converted to intermediate B and C with the help of KBr/g-C_3N_4 and H_2O_2. Finally, the intermediate C could be oxidized further to maleic acid. Furthermore, the presence of KBr can also suppress the side reactions to form SA and FRO.

The influence of the g-C_3N_4 support on the reaction was compared with others such as KBr-doped CeO_2 and KBr-doped TiO_2 catalysts (Entries 15 and 16 in Table 1). These catalysts afforded 9.5% and 40.9% MA yields, respectively. The low selectivity of MA with KBr/CeO_2 as catalyst may be caused by production of by-products. According to the report of Knight *et al*. (1990), besides the desired C4 products (MA, SA, and FRO), furfural oxidation can also produce many by-products such as acetic acid and humins. In the present experiment, the acetic acid was also detected, and it may have originated from the products via deep oxidation of C4 products. Thus, it is proposed that the production of by-products is the main reason for low product yield and low selectivity. This observation indicates that the catalyst support can affect the furfural oxidation reaction pathways. Furthermore, the KBr/g-C_3N_4 showed better activity than a mechanical mixing of KBr and g-C_3N_4 (Entry 9 in Table 1, 47.3% MA yield), which can also indicate the presence of synergistic effect between KBr species and g-C_3N_4 support.

To evaluate the catalytic activity of K and Br, the results of the leaching experiment were analyzed. When the filtrate (Table 1, entry 18) was used as catalyst and solvent, the yield of MA and SA were 25.5% and 18.8%, respectively. Comparing with the blank experiment (Table 1, entry 17), the MA yield increased and SA yield decreased, which may have been caused by a little leaching of K^+ and Br^- after hot-filtration. Furthermore, the 63.2% MA yield could be obtained with catalyst after hot-filtration, which implied that the catalyst activity decreased, which may have been due to the leaching of K^+ and Br^-.

Table 1. Effect of the Different Catalysts on the Synthesis of MA, FRO, and SA from Furfural

Entry	Catalyst	Furfural Conversion (%)	Yield (%)		
			MA	FRO	SA
1	KBr[a]	>99	31.65	-	-
2	KOH[a]	>99	37.10	23.34	20.59
3	KNO_3[a]	>99	12.19	25.23	27.67
4	KCl[a]	>99	22.99	3.55	8.36
5	KBr-KOH[b]	>99	68.04	-	-
6	NaOH[a]	>99	36.14	21.50	3.30
7	KBr-NaOH[c]	>99	61.86	-	-
8	NaBr-NaOH[d]	>99	32.31	-	-
9	KBr-g-C_3N_4[e]	>99	47.31	-	-
10	g-C_3N_4[a]	>99	16.82	27.01	24.72
11	KBr/g-C_3N_4[a]	>99	70.40	-	-
12	KOH/g-C_3N_4[a]	>99	16.15	30.65	44.07
13	KCl/g-C_3N_4[a]	>99	21.12	26.19	22.41
14	KNO_3/g-C_3N_4[a]	>99	13.32	27.48	32.58
15	KBr/CeO_2[a]	>99	9.50	-	-
16	KBr/TiO_2[a]	>99	40.91	-	-
17	blank	>99	17.33	-	26.91
18	Filtrate [f]	>99	25.46	-	18.75
19	KBr/g-C_3N_4[f]	>99	63.25	-	-

Reaction conditions:
[a]100 °C, 180 min, 2 mL water, 1 mL H_2O_2, 1 mmol furfural, and 50 mg catalyst;
[b]100 °C, 180 min, 2 mL water, 1mL H_2O_2, 1 mmol furfural, 50 mg KBr, and 50 mg NaOH;
[c]100 °C, 180 min, 2 mL water, 1 mL H_2O_2, 1 mmol furfural, 20 mg KBr, and 25 mg NaOH;
[d]100 °C, 180 min, 2 mL water, 1 mL H_2O_2, 1 mmol furfural, 50 mg NaBr, and 50 mg NaOH; and
[e]100 °C, 180 min, 2 mL water, 1 mL H_2O_2, 1 mmol furfural, 50mg KBr, and 50 mg g-C_3N_4.
[f] hot-filtration experiment.

Effect of Reactant on Producing MA, SA, and FRO

To investigate the effect of the reactant on the KBr/g-C_3N_4 reaction system, three furan substrates were studied (Table 2). A 64.8% MA yield was obtained when using 2-furoic acid as the starting substrate (Entry 4 in Table 2). The 19.1% SA yield could be obtained with FRO as substrate (Entry 3 in Table 2). According to the report of Xiang *et al*. (2016), FRO may have undergone isomerization to afford hydroxyfuran and then rearrangement to 2(3H)-furanone, which can be oxidized to SA in the presence of hydrogen peroxide. When the substrate was 5-HMF (Entry 2 in Table 2), the MA yield decreased to 1.3%, while a 44.9% SA yield was obtained. Based on the analysis, this reaction system may be suitable for furfural and 2-furoic acid substrates. Furthermore, using KBr (Entry 5 in Table 2) and KOH (Entry 6 in Table 2), the MA yields were 24.6% and 23.9%, respectively. Similarly, improved MA yields were obtained using 2-furoic acid with the KBr/g-C_3N_4 catalyst. Hence, additional work focused on furfural as the starting substrate to study how other reaction conditions affected MA production.

Table 2. The Effect of Substrate on Chemical Yields of MA, SA, and FRO

Entry	Substrate	Yield of products (%)		
		MA	SA	FRO
1	Furfural	69.72	-	-
2	5-HMF	1.33	44.94	-
3	FRO	-	19.14	-
4	2-Furoic acid	64.76	5.70	-
5	2-Furoic acid	24.58	-	6.06
6	2-Furoic acid	23.87	-	-

Reaction conditions:
entry 1 to 4: 50 mg KBr/g-C_3N_4;
entry 5: 50 mg KBr;
entry 6: 50 mg KOH;
All reactions were conducted at 100 °C for 180 min with 1 mmol substrate and 1 mL H_2O_2.

Effect of Water Contents, Reaction Temperature, and Reaction Time on MA Production

KBr-doped g-C_3N_4 was the most efficient catalyst for furfural oxidation to MA (Entry 11 in Table 1). Hence, KBr/g-C_3N_4 was used to investigate the effect other critical reaction parameters, such as water content, reaction temperature, and retention time. Controlling the amount of water in the reaction medium was critical in the resulting MA yield (Li *et al.* 2017). As can be seen in Fig. 4A, the MA yield increased to 70.0% when the water in the reaction system was increased to 2 mL (*i.e.*, 0.67 (v/v) water in the medium). The MA yield decreased slightly when the reaction medium contained 0.75 to 0.80 (v/v) water. However, the MA yield decreased appreciably when the reaction medium had less than 0.60 (v/v) water or greater than 0.80% (v/v) water. In these cases, when the molar ratio of H_2O_2 to furfural was held constant, the reason for the decreasing MA yield may be the adsorption of additional water molecules onto the catalyst, which prevented the furfural from contacting the catalyst surface.

The effect of reaction temperature is shown in Fig. 4B. At 100 °C, the MA yield was higher than they yields obtained when the reactions were performed at 60 to 90 °C. As the reaction temperature increased, more gas bubbles were observed in the sealed glass tubes, which indicated that higher reaction temperatures accelerated H_2O_2 decomposition. When the temperature was further increased to 110 °C, the MA yield decreased. Hence, 100 °C was determined to be the optimal reaction temperature.

In the case of furfural conversion, the reaction time had the greatest effect with respect to MA yield (Fig. 4C). The catalytic results show that MA yield increased from 27.3% to 70.4% as the reaction time increased from 30 to 180 min; the MA yields remained constant for 180 to 210 min. Hence, the amount of MA produced was stable in the catalytic system after 180 min of reaction time.

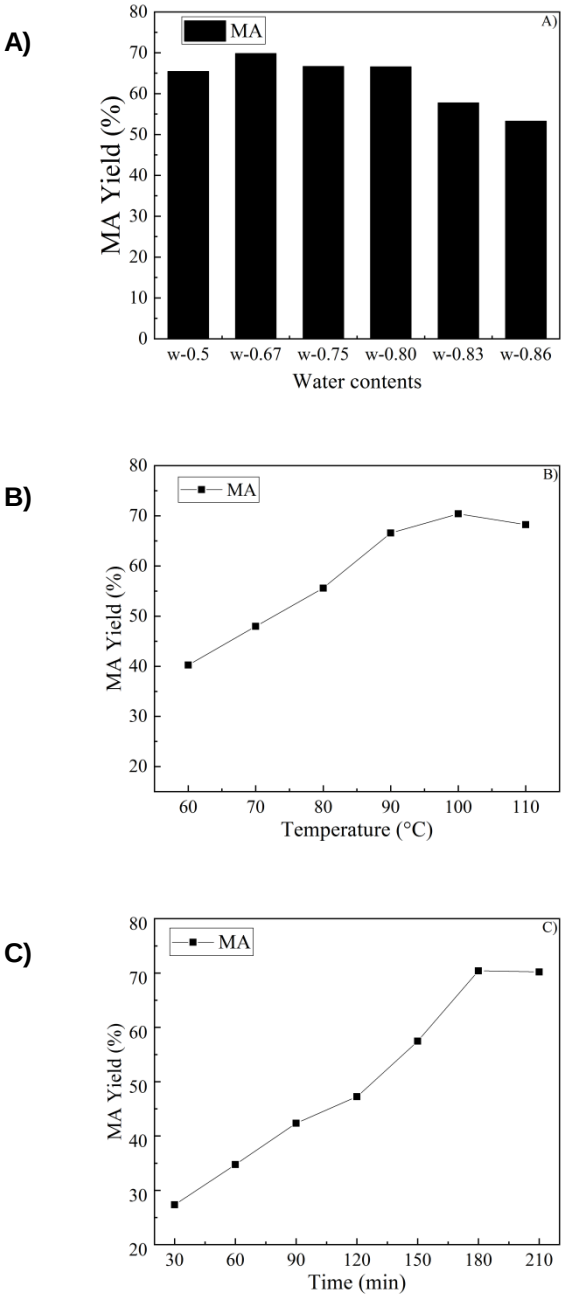

Fig. 4. A) Effect of water in the reaction medium on MA production (v/v ratio); B) effect of reaction temperature on MA production; and C) effect of reaction time on MA production (reaction conditions (unless otherwise specified): 1 mmol (96 mg) furfural, 1 mL H_2O_2, 2 mL water (0.67 (v/v)), and 50 mg KBr/g-C_3N_4 catalyst at 100 °C for 180 min)

Recyclability of the Composite Catalyst

The reusability of the catalyst is an important aspect for its industrial use. The KBr/g-C_3N_4 catalyst was selected to evaluate whether it could be recycled and reused. After every reaction cycle, the catalyst was separated from the liquid products by filtration and washed several times with distilled water. The washed catalyst was then dried in an

oven at 80 °C before reuse in the next cycle. The MA yield decreased slightly after two cycles (Fig. 5). The MA yield dramatically decreased after three cycles, which was postulated to be due to the loss of KBr from the g-C_3N_4 support. The SA and FRO yields increased at the same time as the MA yield decreased. It was hypothesized that the appearance of SA and FRO was due to the influence of leaching of KBr and the presence of g-C_3N_4, which was demonstrated by the result (Entries 10 and 11 in Table 1). The spent KBr/g-C_3N_4 was characterized by XRD (Fig. S4, SI) and TEM-EDS (Fig. S5, SI). As shown in Fig. S4, compared with fresh KBr/g-C_3N_4, the intensity of the corresponding peaks in spent KBr/g-C_3N_4 disappeared, which can be attributed to the leaching of K or Br in the catalyst during reaction. In addition, TEM-EDS (Fig. S5 and Table S2) was used to examine the degradation of the spent catalyst. From the TEM-EDS analysis, the amount of K^+ slightly decreased, whereas Br^- was rarely detected. Next, the spent catalyst was regenerated by calcination; however, regeneration by calcination did not restore the catalyst's performance. The yield of MA increased from 22.8% to 64.7% after regeneration by adding KBr into the used catalyst and calcination, which indicated the catalytic deactivation was primarily due to the leaching of Br^-.

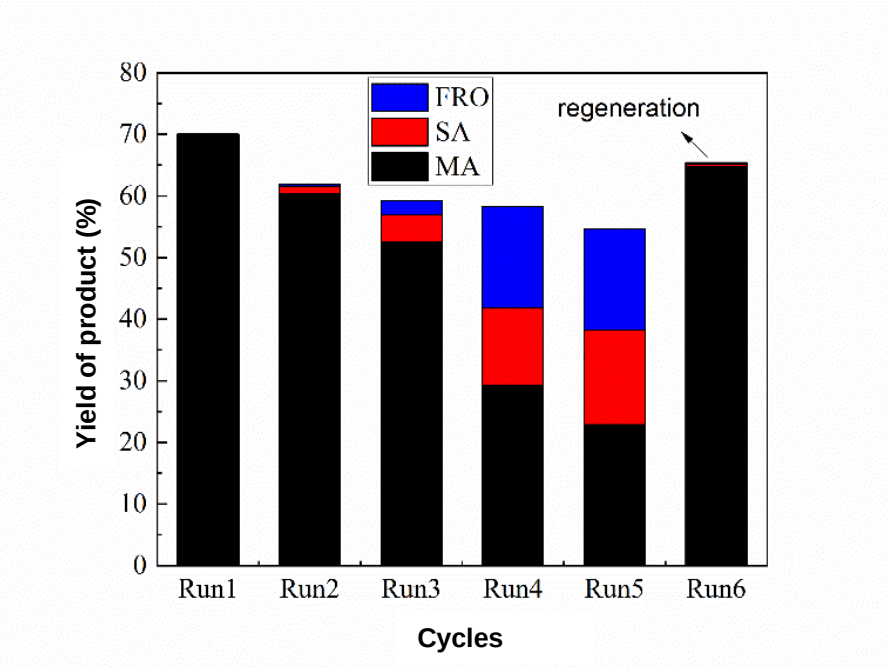

Fig. 5. Reusability of KBr/C_3N_4 catalyst (reaction conditions: 1 mmol (96 mg) furfural, 1 mL H_2O_2, 2 mL water, and 50 mg KBr/g-C_3N_4 at 100 °C for 3 h)

CONCLUSIONS

1. A simple and efficient catalytic system was developed for the oxidation of furfural to maleic acid (MA) using H_2O_2 as the oxidant, water as part of the reaction medium, and KBr-KOH or KBr/g-C_3N_4 as the catalyst.
2. The synergistic interaction of KBr and KOH was crucial for higher MA yield in the homogeneous system, whereas the KBr/g-C_3N_4 can be used as a heterogeneous catalyst. Under mild reaction conditions, the optimum MA yields were 68.0% and

70.0% when catalyzed by KBr-KOH and KBr/g-C_3N_4, respectively. Meanwhile, the reaction temperature, the water content in the reaction medium, and the reaction time were the key reaction conditions for enhancing MA yield.

3. When comparing KBr to KCl, KNO_3, and KOH on the g-C_3N_4 support, there was a synergism between KBr and g-C_3N_4. The g-C_3N_4 support can be used as a Brønsted base to ionize H_2O_2 to HOO^- in the aqueous reaction medium. The presence of KBr is postulated to suppress the side reaction products of 2-buten-1,4-olide (FRO) and succinic acid (SA) while enhancing MA yield.
4. The recovered KBr/g-C_3N_4 catalyst can be recycled for at least three cycles before the MA yield is impaired. The KBr/g-C_3N_4 catalyst can be regenerated.

ACKNOWLEDGMENTS

This study was financially supported by the State Key Program of the National Natural Science Foundation of China (Grant No. 51536009); the Transformational Technologies for Clean Energy and Demonstration, Strategic Priority Research Program of the Chinese Academy of Sciences (Grant No. XDA 21060101); and the National Key Technology R&D Program of China (Grant No. 2015BAD15B06).

REFERENCES CITED

Alonso-Fagundez, N., Granados, M. L., Mariscal, R., and Ojeda, M. (2012). "Selective conversion of furfural to maleic anhydride and furan with VO(x)/Al_2O_3 catalysts," *ChemSusChem* 5, 1984-1990. DOI: 10.1002/cssc.201200167

Alonso-Fagúndez, N., Agirrezabal-Telleria, I., Arias, P. L., Fierro, J. L. G., Mariscal, R., and Granados, M. L. (2014). "Aqueous-phase catalytic oxidation of furfural with H_2O_2: High yield of maleic acid by using titanium silicalite-1," *RSC Advances* 4, 54,960-54,972. DOI: 10.1039/C4RA11563E

Araji, N., Madjinza, D. D., Chatel, G., Moores, A., Jérôme, F., and De Oliveira Vigier, K. (2017). "Synthesis of maleic and fumaric acids from furfural in the presence of betaine hydrochloride and hydrogen peroxide," *Green Chemistry* 19(1), 98-101. DOI: 10.1039/c6gc02620f

Badovskaya, L. A., Poskonin, V. V., and Ponomarenko, R. I. (2014). "Effect of acid-base properties of the medium on the reactions in the 2-furaldehyde-H_2O_2-H_2O system with and without $VOSO_4$," *Russian Journal of General Chemistry* 84, 1133-1140. DOI: 10.1134/S1070363214060140

Choudhary, H., Nishimura, S., and Ebitani, K. (2013). "Metal-free oxidative synthesis of succinic acid from biomass-derived furan compounds using a solid acid catalyst with hydrogen peroxide," *Applied Catalyst A: General* 458, 55-62. DOI: 10.1016/j.apcata.2013.03.033

Cui, L., Ding, X., Wang, Y., Shi, H., Huang, L., Zuo, Y., and Kang, S. (2017). Facile preparation of Z-scheme WO_3/g-C_3N4 composite photocatalyst with enhanced photocatalytic performance under visible light," *Applied Surface Science* 391, 202-210. DOI: 10.1016/j.apsusc.2016.07.055

Danon, B., van der Aa, L., and de Jong, W. (2013). "Furfural degradation in a dilute acidic and saline solution in the presence of glucose," *Carbohydrate Research* 375, 145-152. DOI: 10.1016/j.carres.2013.04.030

Du, Z., Ma, J., Wang, F., Liu, J., and Xu, J. (2011). "Oxidation of 5-hydroxymethyl-furfural to maleic anhydride with molecular oxygen," *Green Chemistry* 13, 554-557. DOI: 10.1039/C0GC00837K

Gao, H., Yan, S., Wang, J., Huang, Y. A., Wang, P., Li, Z., and Zou, Z. (2013). "Towards efficient solar hydrogen production by intercalated carbon nitride photocatalyst," *Physical Chemistry Chemical Physics* 15, 18,077-18,084. DOI: 10.1039/c3cp53774a

Guo, H., and Yin, G. (2011). "Catalytic aerobic oxidation of renewable furfural with phosphomolybdic acid catalyst: An alternative route to maleic acid," *The Journal of Physical Chemistry C* 115(35), 17516-17522. DOI: 10.1021/jp2054712

Knight, E. V., Novick, N. J., Kaplan, D. L., and Meeks, J. R. (1990). "Biodegradation of 2-furaldehyde under nitrate-reducing and methanogenic conditions," *Environmental Toxicology and Chemistry: An International Journal* 9(6), 725-730. DOI: 10.1002/etc.5620090605

Kul'nevich, V. G., and Badovskaya, L. A. (1975). "Reactions of oxo-derivatives of furan with hydrogen peroxide and peroxy-acids," *Russian Chemistry Review* 44, 1256. DOI: 10.1070/RC1975v044n07ABEH002362

Lin, B., Yang, G., Yang, B., and Zhao, Y. (2016). "Construction of novel three dimensionally ordered macroporous carbon nitride for highly efficient photocatalytic activity," *Applied Catalyst B: Environmental* 198, 276-285. DOI: 10.1016/j.apcatb.2016.05.069

Li, X., Ho, B., and Zhang, Y. (2016a). "Selective aerobic oxidation of furfural to maleic anhydride with heterogeneous Mo-V-O catalysts," *Green Chemistry* 18, 2976-2980. DOI: 10.1039/C6GC00508J

Li, X., Lan, X., and Wang, T. (2016b). "Selective oxidation of furfural in a bi-phasic system with homogeneous acid catalyst," *Catalysis Today* 276, 97-104. DOI: 10.1016/j.cattod.2015.11.036

Li, X., Ho, B., Lim, D. S. W., and Zhang, Y. (2017). "Highly efficient formic acid-mediated oxidation of renewable furfural to maleic acid with H_2O_2," *Green Chemistry* 19, 914-918. DOI: 10.1039/C6GC03020C

Podolean, I., Rizescu, C., Bala, C., Rotariu, L., Parvulescu, V. I., Coman, S. M., and Garcia, H. (2016). "Unprecedented catalytic wet oxidation of glucose to succinic acid induced by the addition of *n*-butylamine to a Ru^{III} catalyst," *ChemSusChem* 9, 2307-2311. DOI: 10.1002/cssc.201600474

Rizescu, C., Podolean, I., Cojocaru, B., Parvulescu, V. I., Coman, S. M., Albero, J., and Garcia, H. (2017). "$RuCl_3$ supported on N-doped graphene as a reusable catalyst for the one-step glucose oxidation to succinic acid," *ChemCatChem* 9(17), 3314- 3321. DOI: 10.1002/cctc.201700383

Roa Engel, C. A., Straathof, A. J. J., Zijlmans, T. W., van Gulik, W. M., and van der Wielen, L. A. M. (2008). "Fumaric acid production by fermentation," *Applied Microbiology and Biotechnology* 78(3), 379-389. DOI: 10.1007/s00253-007-1341-x

Samanta, S., and Srivastava, R. (2017). "A novel method to introduce acidic and basic bi-functional sites in graphitic carbon nitride for sustainable catalysis: Cycloaddition,

esterification, and transesterification reactions," *Sustainable Energy and Fuels* 1(6), 1390-1404. DOI: 10.1039/C7SE00223H

Su, F. Z., Mathew, S. C., Lipner, G., Fu, X. Z., Antonietti, M., Blechert, S. and X. Wang, C. (2010). "mpg-C_3N_4-catalyzed selective oxidation of alcohols using O_2 and visible light," *Journal of the American Chemical Society* 132(46), 16,299-16,301. DOI: 10.1021/ja102866p

Takase, M., Zhang, M., Feng, W., Chen, Y., Zhao, T., Cobbina, S. J., Yang, L., and Wu, X. (2014). "Application of zirconia modified with KOH as heterogeneous solid base catalyst to new non-edible oil for biodiesel," *Energy Conversion and Management* 80, 117-125. DOI: 10.1016/j.enconman.2014.01.034

Wang, J., Li, W., Wang, H., Ma, Q., Li, S., Chang, H.-m., and Jameel, H. (2017). "Liquefaction of kraft lignin by hydrocracking with simultaneous use of a novel dual acid-base catalyst and a hydrogenation catalyst," *Bioresource Technology* 243, 100-106. DOI: 10.1016/j.biortech.2017.06.024

Wojcieszak, R., Santarelli, F., Paul, S., Dumeignil, F., Cavani, F., and Gonçalves, R. V. (2015). "Recent developments in maleic acid synthesis from bio-based chemicals," *Sustainable Chemical Processes* 3(1), 9. DOI: 10.1186/s40508-015-0034-5

Xiang, X., Zhang, B., Ding, G., Cui, J., Zheng, H., and Zhu, Y. (2016). "The effect of $Mg(OH)_2$ on furfural oxidation with H_2O_2," *Catalyst Communications* 86, 41-45. DOI: 10.1016/j.catcom.2016.08.013

Xu, S., Pan, D., Wu, Y., Song, X., Gao, L., Li, W., and Xiao, G. (2018). "Efficient production of furfural from xylose and wheat straw by bifunctional chromium phosphate catalyst in biphasic systems," *Fuel Processing Technology* 175, 90-96. DOI: 10.1016/j.fuproc.2018.04.005

Yang, Y., Geng, L., Guo, Y., Meng, J., and Guo, Y. (2017). "Easy dispersion and excellent visible-light photocatalytic activity of the ultrathin urea-derived g-C3N4 nanosheets," *Applied Surface Science* 425, 535-546. DOI: 10.1016/j.apsusc.2017.06.323

Zhang, W., Zhu, Y., Niu, S., and Li, Y. (2011). "A study of furfural decarbonylation on K-doped Pd/Al_2O_3 catalysts," *Journal of Molecular Catalysis A: Chemical* 335, 71-81. DOI: 10.1016/j.molcata.2010.11.016

Zhang, Y., Liu, J., Wu, G., and Chen, W. (2012). "Porous graphitic carbon nitride synthesized *via* direct polymerization of urea for efficient sunlight-driven photocatalytic hydrogen production," *Nanoscale* 4, 5300-5303. DOI: 10.1039/c2nr30948c

Zhang, M., Bai, X., Liu, D., Wang, J., and Zhu, Y. (2015). "Enhanced catalytic activity of potassium-doped graphitic carbon nitride induced by lower valence position," *Applied Catalyst B: Environmental* 164, 77-81. DOI: 10.1016/j.apcatb.2014.09.020

Zhang, T., Li, W., Xu, Z., Liu, Q., Ma, Q., Jameel, H., Chang, H.-m., and Ma, L. (2016). "Catalytic conversion of xylose and corn stalk into furfural over carbon solid acid catalyst in gamma-valerolactone," *Bioresource Technology* 209, 108-114. DOI: 10.1016/j.biortech.2016.02.108

Article submitted: February 3, 2019; Peer review completed: April 16, 2019; Revisions accepted: May 1, 2019; Published: May 2, 2019.
DOI: 10.15376/biores.14.3.5025-5044

APPENDIX

SUPPLEMENTARY INFORMATION

Table S1. Element Composition of g-C_3N_4 and KBr/g-C_3N_4

	Atomic ratio (%)					Basicity (mmol/g)	S_{BET} (m^2/g)
Sample	C	N	O	K	Br		
g-C_3N_4	50.08	49.92	-	-	-	1.67	220.1
KBr/g-C_3N_4	48.92	40.58	2.50	7.39	0.61	1.61	13.2

Table S2. Element Composition of Fresh KBr/g-C_3N_4, Spent KBr/g-C_3N_4 and Regenerated KBr/g-C_3N_4 by TEM-EDS

	Wt. (%)		
Sample	N	K	Br
[a] KBr/g-C_3N_4	57.13	25.77	17.10
[b] S-KBr/g-C_3N_4	70.58	29.04	0.38
[c] R-KBr/g-C_3N_4	41.81	43.54	14.65

[a]Fresh KBr/g-C_3N_4 ; [b]used KBr/g-C_3N_4; and [c]regenerated KBr/g-C_3N_4

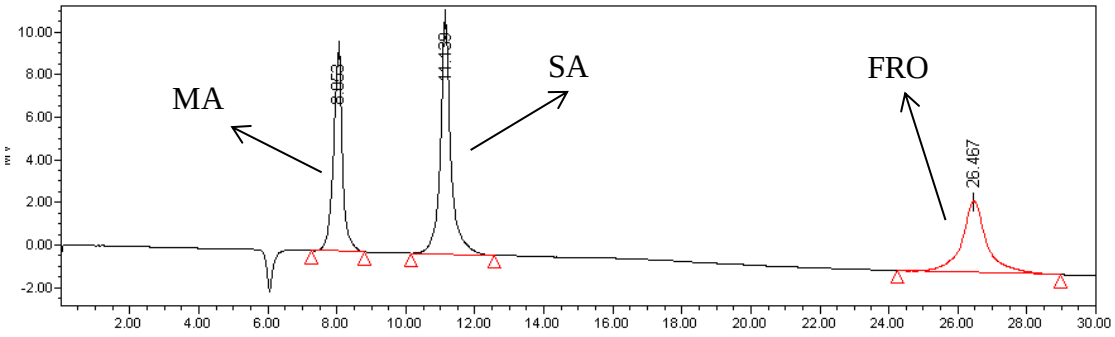

Fig. S1. The HPLC chromatogram of the reaction mixture from furfural oxidation. Retention time: maleic acid, 8.053 min; SA, 11.139 min; FRO, 26.467 min

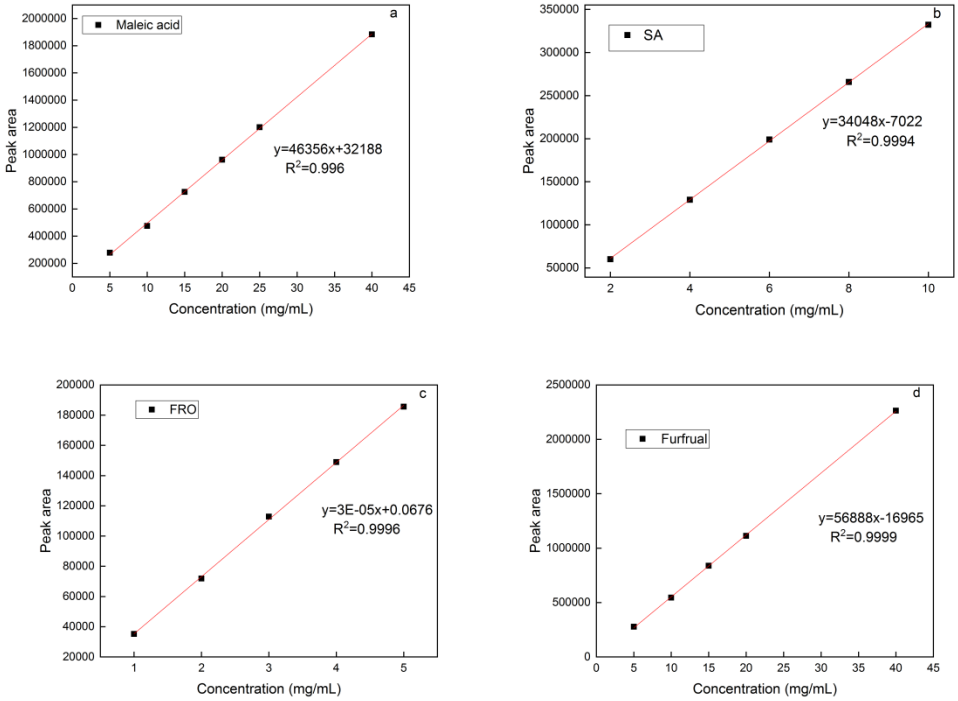

Fig. S2. Standard curve of products and substrate: (a) MA, (b) SA, (c) FRO, and (d) furfural

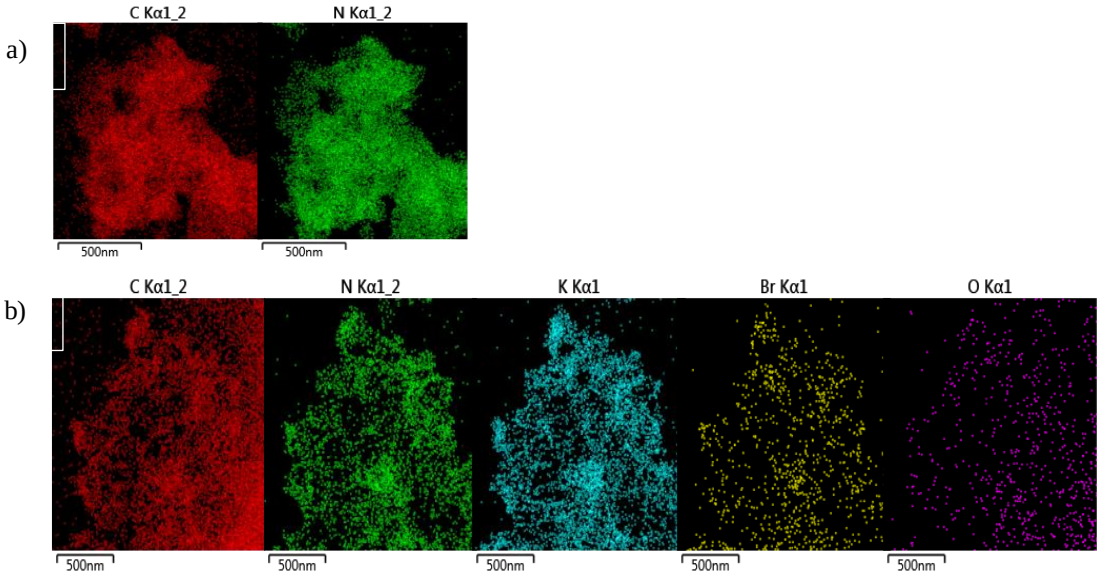

Fig. S3. Element map images of (a) g-C_3N_4 and (b) KBr/g-C_3N_4

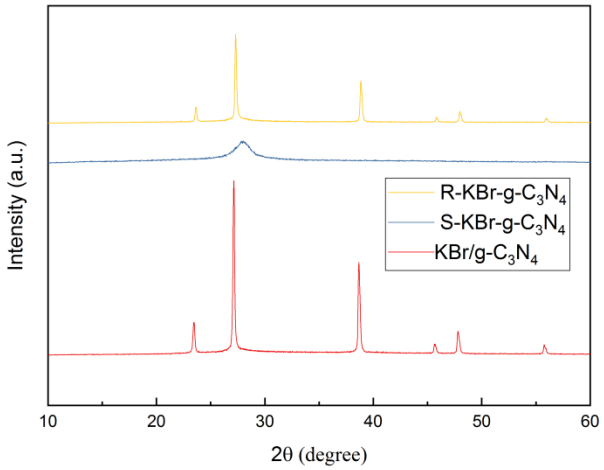

Fig. S4. XRD spectra of fresh KBr/g-C_3N_4, spent KBr/g-C_3N_4 and regenerated KBr/g-C_3N_4

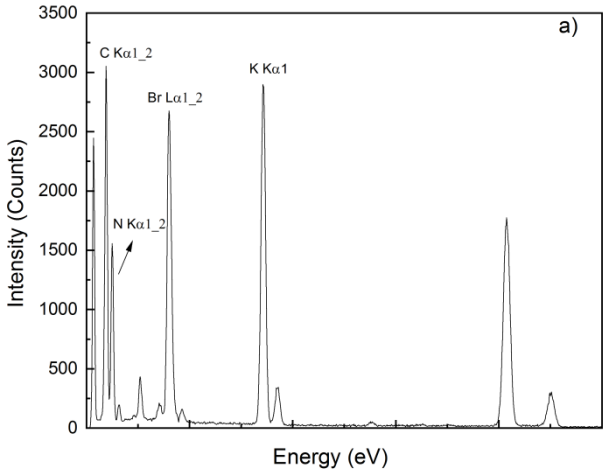

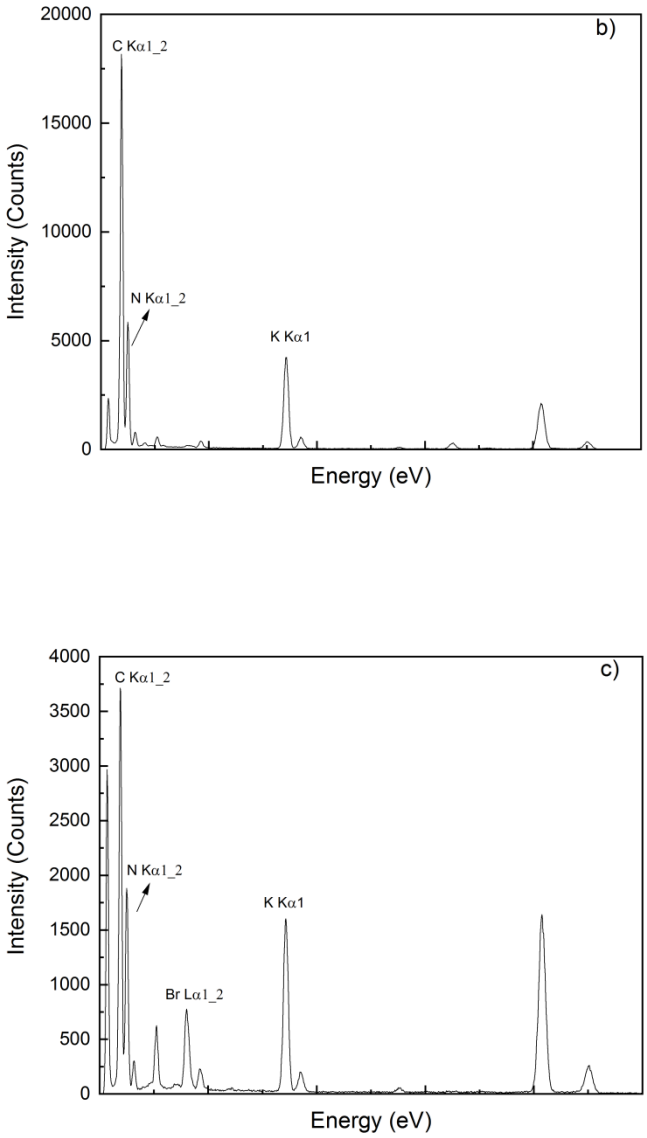

Fig. S5. TEM-EDS spectrum of (a) fresh KBr/g-C_3N_4, (b) spent KBr/g-C_3N_4, and (c) regenerated KBr/g-C_3N_4

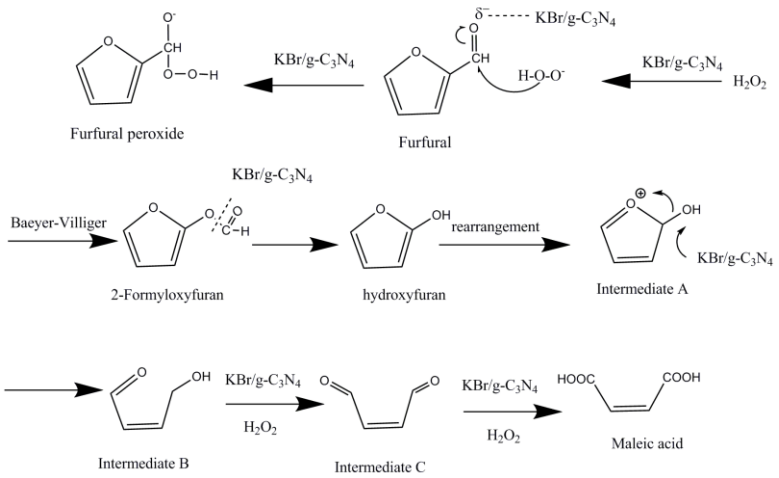

Fig. S6. Proposed reaction pathway and the role of KBr/g-C_3N_4 for furfural oxidation to MA

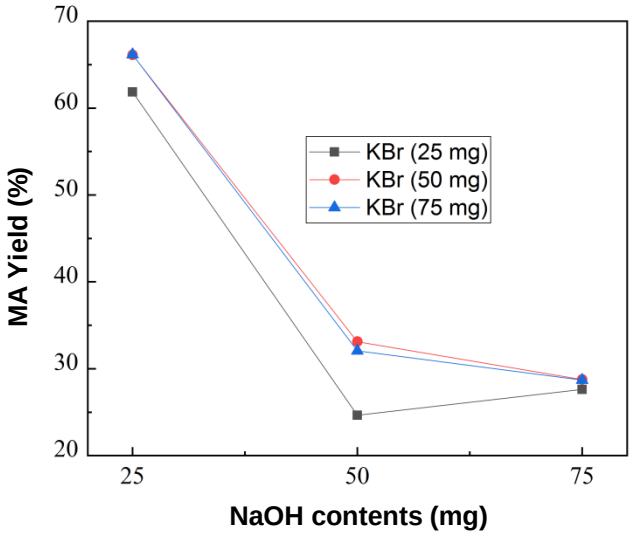

Fig. S7. Effect of KBr/NaOH contents on the oxidation of furfural to MA
Reaction conditions: 1 mmol furfural, 1 mL H_2O_2, 2 mL DIW, 100 °C, 3 h.